# Synergic comanipulation despite underactuated robot

Anja Marx, Marie-Aude Vitrani, Benoˆt Herman, Rˇzvan Iordache, Serge Muller, Guillaume Morel

# Synergic Comanipulation Despite Underactuated Robot

Anja Marx, Marie-Aude Vitrani, Benoît Herman, Răzvan Iordache, Serge Muller and Guillaume Morel

***Abstract*— The possibility to provide an adequate task assistance using underactuated robots for human-robot tool comanipulation is investigated. This novel approach does not take into account any a priori knowledge about user depending parameters however optimizes the robot-user synergy, for instance during US breast examinations. Results show that the examination time can be reduced and a tendency for increasing scanning accuracy using underactuated robots.**

## I. Comanipulation for Medical Applications

Comanipulated devices are systems in which the robot and the user manipulate together the same tool. This paradigm is particularly interesting for medical applications. Indeed, unlike teleoperated systems, comanipulation devices allow the physician to remain with the patient, by directly handling the instruments that perform the gesture. In an ideal comanipulated system, the medical gesture is unchanged with the addition of a robot. The robot acts as a device providing active support to improve performance and to make the gesture safer. Comanipulation devices can be sorted in three categories, in function of the task that they perform.

A first task is to localize and calibrate the robot with respect to the patient. It is based on a typical force control law. If the desired effort applied by the robot is set to zero when the surgeon applies an effort onto the tool, the robot does not resist and so follows the user's gesture. In [5], a force compliance mode allows the surgeon to move the robot in order to locate centers of three pins implanted in a bone and to compute the appropriate location of the shape to be cut. In [6], a robotic system for skin harvesting is presented. When used in the manual mode, the surgeon can move the robot towards the initial pose on skin, then towards the final pose to define the trajectory the robot must follow.

A second class of devices was developed to provide the surgeon with a better feeling of the tool-patient interaction. When the laparoscopic tool holder MC2E is force controlled with a zero desired force, the surgeon can feel the forces exerted on the tissues and organs without being corrupted by the trocar friction forces [8]. In [9], Taylor et al. proposed a steady-hand device for microsurgery. This device allows scaling of interaction forces: forces applied by the surgeon on the eye are much lower than those felt by the surgeon.

This paper focuses on the third category that intends to guide the user by imposing kinematic constraints on the tool. To reach this goal, ancestors of "comanipulated" systems were presented in [1] for neurosurgery and spine surgery. In this paper, Cinquin et al. present two devices allowing to position a mechanical guide through which the surgeon introduces linear operative tools (e.g. drills). The limit of these systems is that the task must be divided into two successive actions—the first one is performed by the robot, and the second one by the surgeon while the robot remains inactive. As a consequence, only static constraints can be generated. Real-time adaptation is impossible. To overcome this, Schneider et al. propose a semi-passive device called "Passive Arm with Dynamic Constraints" (PADyC, [2]). Semi-passive means that any motion of the robot requires the action of the user. Its mechanical design enables to limit the motions of a tool according to a planned task. A geometrical zone is defined in which the surgeon can move freely. When moving out of the zone the surgeon feels forces applied by the robot and aimed at moving him back inside the prescribed zone. This function of geometrical guidance is also proposed in [3] and [4]. Davies et al. present a robot for knee surgery named ACROBOT (Active Constraint ROBOT). The comanipulation does not result from a mechanical constraint but is provided thanks to force control. The robot can be provided with regions of force constraints so that a flat or curved plane can be cut accurately into the bone to allow the prosthetic implant to be subsequently fitted. Furthermore, the robot can also be programmed to prevent any intrusion into adjacent regions, thus avoiding damage to ligaments. The basic idea behind active constraint control is to gradually increase the stiffness of the robot as it approaches the predefined boundary. The same principle is used to control the Surgicobot robot (based on a haptic device) which can be programmed with a desired apparent stiffness within a quite wide range, but without force sensor [4].

To the best of our knowledge, it can be observes that all the systems within this latter class have sufficient actuated degrees of freedom (DOFs) to perform the task without a human user. However, imposing the desired kinematic constraints generally do not require so many actuators. In this paper, we study through an example the possibility to provide the adequate assistance for a comanipulation task with an underactuated robot. The immediate advantage is to have a more compact, less complex system at a lower cost. Careful attention must yet be paid to the system design to obtain the appropriate synergic behavior of the human-robot

This work has been partially funded by ANRT under CIFRE grant $n^o$247/2009.

A. Marx is with GE Healthcare, Buc, France, and with Institut des Systmes Intelligents et de Robotique, Université Pierre et Marie Curie-Paris 6, Paris, France. anja.marx@ge.com

R. Iordache and S. Muller are with GE Healthcare, Buc, France. {razvan.iordache, serge.muller}@ge.com

M.-A. Vitrani, B. Herman and G. Morel are with Institut des Systmes Intelligents et de Robotique, Université Pierre et Marie Curie-Paris 6, Paris, France. {marie-aude.vitrani, benoit.herman, guillaume.morel}@isir.upmc.fr

collaboration.

The rest of the paper presents the particular medical context of breast cancer detection and the general comanipulation strategy in section II. Then, in section III, the chosen task and the proposed system are described. Finally, experimental results and discussions are detailed in section IV.

## II. Novel Comanipulation Strategy for US Probe Guiding

### A. Clinical Context and Requirements

Early detection examinations for breast cancer are typically conducted using digital breast tomosynthesis (DBT), a new 3D X-ray imaging device that overcomes one of the main limitations of the (2D) mammography, tissue overlapping. Given the situation that a DBT scan shows multiple suspicious lesions within a patient's breast, the investigator usually calls for a supplementary ultrasound (US) manual scan. This complementary examination aims at identifying tumors among the suspicious lesions. The big challenge of this additional examination is to find the previously identified suspicious zone in the US images of the now uncompressed breast. Note that during DBT scanning the patients breast is compressed between a paddle and a detector, in order to avoid image noise due to patient movements like breathing. This is depicted in figure 1. However, for a successful US examination, it is usually necessary to decompress the patient's breast, because the compression paddles used in common DBT scans are not US compatible due to material characteristics. In addition to the difficult localization of the lesion, the mental matching between both image modalities gets more complicated because US examinations are mostly conducted hours or even days after the primary DBT scan, when a radiologist has analyzed and interpreted the DBT images.

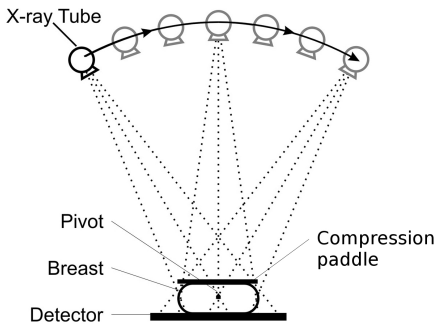


Fig. 1. DBT setup: The X-ray tube turns around its pivot point to scan the breast from different angles, which is compressed between the detector and a paddle.

A first way to make the US examination easier is to use novel US compatible compression paddles. This allows a US examination immediately after the DBT scan, while the breast remains compressed and so keeps its shape. The DBT and US images show hence breast planes of the same breast pose, which facilitates the mental matching between both image modalities and the lesion localization. The surgeon task is then to find and scan the suspicious zone while maintaining the contact between the probe and the paddle. This task has 4 DOFs, as shown in figure 2 and detailed in section III below: two translations of the probe tip on the paddle, assumed to be planar, one rotation along the normal of the paddle surface, and a second rotation around the intersection line of the paddle surface and the US image plane.

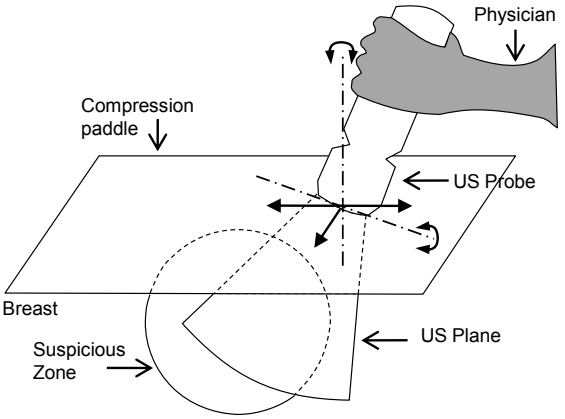


Fig. 2. Compressed Breast Scan with US Probe

From the physician point of view, the US scan remains complex even with this first improvement. He/she has still to mentally reconstruct the shape and 3D-location of the suspicious lesion from the DBT images, in order to position the probe. This mathematical and geometric computation could be performed easily by a computer. This information could then be sent to a robot, that would guide the doctor towards the lesion with an expected increase of both speed and accuracy.

### B. Purpose of Underactuation

The physician's arm and hand possess enough DOFs to move the probe while maintaining the contact with the paddle. The main difficulty to overcome is to locate the lesion with respect to the US plane. The most relevant pieces of information that would ease this location are the relative distance and the direction in which the probe should be moved to reach the target. This indication can be given by a force transmitted by the robot on the probe. A 3 DOFs haptic robot is therefore sufficient to provide the required assistance, although it is underactuated with respect to the 4 DOFs task—exerting a force on a point of the probe is clearly not sufficient to perform the task.

This force should be set to zero while the US plane intersects a lesion, or more generally a region of interest (ROI), in order to let the examiner translate and/or rotate the US probe freely. It must then increase progressively to indicate that he/she is moving away from the ROI, but with maintaining the possibility to scans regions outside the lesion.

An important requirement of the application is that the physician must be free to choose the 2D cross-section observed with the US-Probe to analyze the lesion. This means that he/she must be able to control either the position or the orientation of the probe (or both). The robot feedback should hence be given without any a priori knowledge of the users' strategy to bring back the US plane inside the ROI. Although it is not the only solution, underactuation can ensure this freedom of motion, under certain conditions to guarantee the human-robot-tool system stability. This is discussed in the next section, after the modelling of the US scan task and the computation of the required force.

## III. Task Description and System Overview

### A. US Scan Modelling

The general model of the system is illustrated in figure 3.

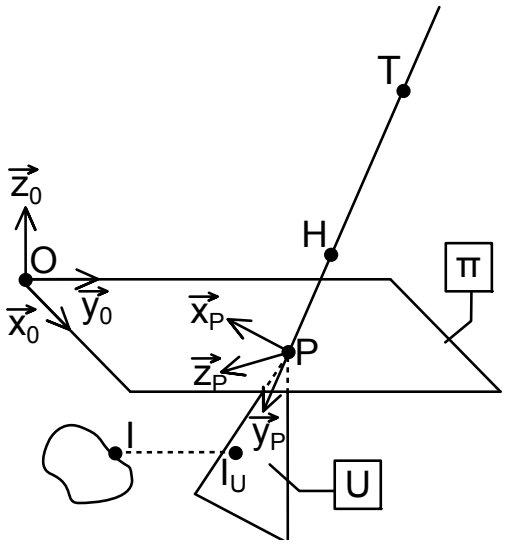


Fig. 3. Geometrical modelling

The ultrasound beam is assumed to be a plane denoted $U$ which was experimentally validated in [10]. Furthermore, the paddle is said by the constructor to be a plane denoted $\Pi$. In the next, the two following orthonormal coordinate frames are used :

- $\mathcal{F}_P = (P, \vec{x}_P, \vec{y}_P, \vec{z}_P)$, the frame attached to the probe with $\vec{z}_P$ the vector normal to the ultrasound plane and $P$ the origin of the US-ray.
- $\mathcal{F}_0 = (O, \vec{x}_0, \vec{y}_0, \vec{z}_0)$, the frame attached to the paddle with $O$ a point belonging to the plane $\Pi$ and $\vec{z}_0$ the vector normal to it.

Furthermore, the ultrasound probe is handled by the human user at point $H$ in such a way that $\overrightarrow{PH} = -||\overrightarrow{PH}||\vec{y}_P$. The robot can apply a force on the probe at point $T$, defined as $\overrightarrow{PT} = -||\overrightarrow{PT}||\vec{y}_P$. The point of the suspicious lesion which minimizes the distance to the ultrasound plane $U$ is denoted $I$. Its projection on the ultrasound plane is denoted $I_U$.

### B. Computation of Desired Force

In most surgical applications, the tool (e.g. saw, drill) must be kept inside a prescribed zone. When it approaches the border of the "free motion" zone, a common comanipulation scheme will increase rapidly the force to reach a value that locks any further motion towards the border. As stated above, in the present application, the doctor might want to scan regions around the ROI. Consequently, the robot should not prevent the user from moving out of the ROI. It should only apply a force that increases proportionally with the distance $\vec{d} = \overrightarrow{II_U}$ between the US plane and the target. This force

$$\vec{F} = k\vec{d} \tag{1}$$

simulates the behavior of an ideal spring with a stiffness $k$.

The vertical component of this force along $\vec{z}_0$ should be set to zero in order to avoid any disturbance on the contact constraint. Therefore,

$$\vec{F} = k\left[\vec{d} - (\vec{d}\cdot\vec{z}_0)\vec{z}_0\right]. \tag{2}$$

This spring force should also be damped to maintain stability even under a rapid change of the distance $\vec{d}$. This can occur in configurations where a small rotation of the probe creates a large variation of the distance. Thus, the force becomes

$$\vec{F} = k\left[\vec{d} - (\vec{d}\cdot\vec{z}_0)\vec{z}_0\right] + c\frac{\Delta\vec{d}}{\Delta t}, \tag{3}$$

where $c$ is the damping coefficient.

Moreover, a second damping factor was included to avoid end-effector oscillations. This is required by technical limitations of the robot chosen for the experimental setup (see section IV below). It is proportional to the end-effector's velocity $\vec{v}_T$ computed over the same period $\Delta t$:

$$\vec{F} = k\left[\vec{d} - (\vec{d}\cdot\vec{z}_0)\vec{z}_0\right] + c\frac{\Delta\vec{d}}{\Delta t} + c_T\vec{v}_T. \tag{4}$$

Finally, a constant gravity compensating force was added to avoid the user to carry a too heavy weight and to prevent that the US probe falls down once the user releases the probe. The final force is then

$$\vec{F} = k\left[\vec{d} - (\vec{d}\cdot\vec{z}_0)\vec{z}_0\right] + c\frac{\Delta\vec{d}}{\Delta t} + c_T\vec{v}_T + mg\vec{z}_0, \tag{5}$$

where the mass $m$ was estimated manually according to the best haptic sensation.

### C. Robot-Probe Interaction

One can state two possible configurations for the relative placement of the hand and robot end-effector on the probe. The user might grasp the probe *above* the robot end-effector (see figure 4) or *below* (see figure 5). The second solution, called hereafter "direct probe grasp", seems to be more suitable because the physician can still grasp the probe at its bottom end with few interference from the robot. Unfortunately, this leads to an unstable behavior, as explained below.

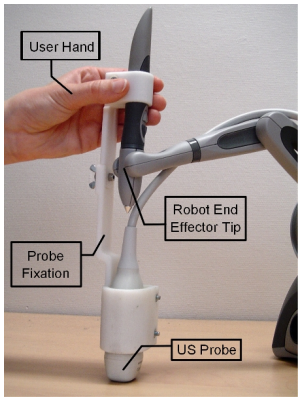


Fig. 4. Tool handling with hand above robot end-effector.

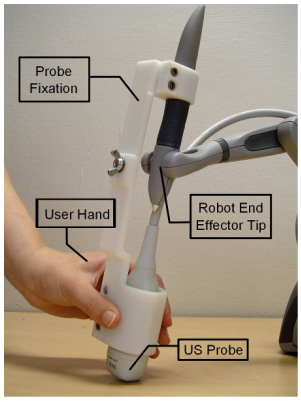


Fig. 5. Tool handling with hand below robot end-effector.

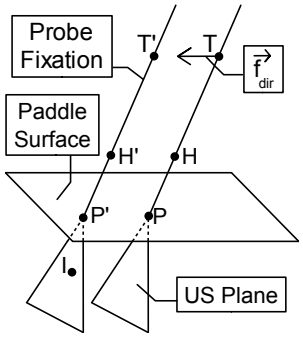


Fig. 6. Probe orientation and position for stiff grasps.

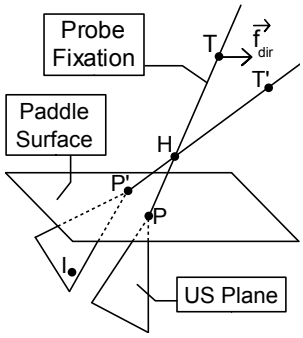


Fig. 7. Probe orientation and position for soft grasps.

*1) Direct Probe Grasp:* In case of directly grasping the probe, the users' stiffness requires two different control laws to accomplish the scanning task around a ROI.

*Stiff Grasp*: The users' hand is tightened and the stiff grasp does not permit any probe movement or sliding within the hand. To change the probe's pose to a desired position the user follows the direction indicated by the robot. Hence a force in the direction of the desired probe position, towards the POI $I$, is applied. Figure 6 sketches the geometrical model for this case. $H$ represents the users' *h*and, $P$ the origin of the US *p*lane and $T$ the robot end-effector *t*ip. To achieve a moving of the US plane $U$ for a stiff user grasp, a force in $f_{dir}$ has to be applied in $T$. Note, that due to the robot architecture, it can only apply forces in $T$. As the probe is rigidly attached to $T$ and the user has a stiff grasp, that means follows the robot indications, $f_{dir}$ causes a hand movement towards $I$. This results in a new position for $T$ and $P$, $T'$ and $P'$ respectively, where $U$ intersects $I$.

*Soft Grasp*: The users' hand is relaxed and permits the probe to slide within the hand when the robot applies a force. Hence, once the robot moves, the human grasp provokes a pivot point of the hang-up at the height of the fingers. This means, the probe orientation changes with every end-effector shift. Figure 7 displays the geometrical representation for this case. To achieve an intersection of the US plane and the POI, the robot has to apply a force $f_{dir}$ in the opposite direction as for a stiff grasp. This is due to the fact that $H$ functions as a rotation point because of the soft grasp.

One can state two different robot commands for a direct probe handle which differ only in a sign. The choice of the control law is hence highly dependent on the users' stiffness, i.e. its soft or stiff grasp. As this is not a priori known, the wrong choice of the force direction can result in an unstable system which is not appropriate for any system.

*2) End-effector Grasp:* In case of manipulating the imaging tool above the robot end-effector, one can note that in both cases the direction of the applied force remains the same.

*Stiff Grasp*: Similar to the case described above, a stiff grasp does not permit any end-effector movement or sliding within the hand. The user keeps the end-effector tight within the hand and follows the direction indicated by the robot. As the probe is rigidly attached to the end-effector, its pose changes with any end-effector movement. To approach the US plane to $I$, a force is hence applied in $T$ in the direction of the desired probe position. Figure 8 sketches this principle.

*Soft Grasp*: The user softly holds the end-effector and permits to slide within the hand when the robot applies a force. Hence, once the robot moves, the human grasp provokes a pivot point at the height of the fingers. This means, the probe orientation is changed whereas the hand position remains relatively stable. To sight a POI, the robot applies a force in direction of the POI to change the probe orientation. Figure 9 displays the geometrical model for this case.

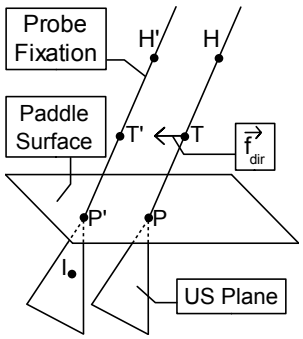


Fig. 8. Probe orientation and position for stiff grasps.

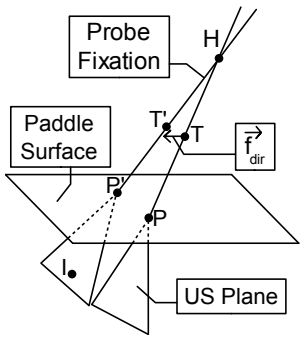


Fig. 9. Probe orientation and position for soft grasps.

This analysis for a direct end-effector grasp shows that independent of the users' stiffness the returned force direction remains the same to successfully accomplish the scanning task. This is the main reason why we chose to implement this solution. Furthermore, the returned force indicates the user a problematic probe state, i.e. a too large distance to the POI or ROI, and at the same time proposes a solution to better perform the actual task without restricting the user movement. As described in section II, this behavior was one of the main requirements for this haptic system.

## IV. Experimental Validation

### A. Setup

We choose to use a PHANToM Omni robot, distributed by SensAble Technologies, Inc., Woburn, MA. It is a commercially available 6DOFs haptic robot. Three DOFs are actuated to position a point of the end-effector. The three other DOFs (orientation of the end-effector with respect to the robot base) are not actuated. This robot is designed to produce a force feedback at its end-effector tip. The PHANToM Omni robot hence satisfies the demand of having less steerable degrees than would be needed to automatically execute the task. In addition it is easy to handle and has low friction.

To manipulate the US probe, a probe fixation was designed to rigidly mount the probe on the robot end-effector, figure 10. This implies that any force applied on the robot end-effector has equally an impact on the probe. In the current work, we made use of a simple cardiac US probe as it is small and light, so the robot is strong enough to carry the probe and its fixation.

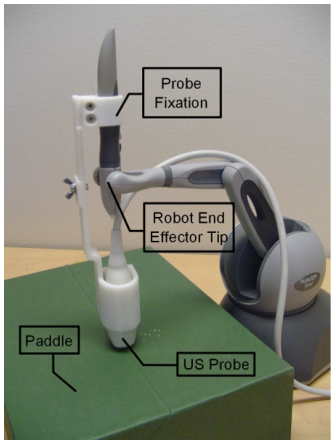


Fig. 10. Experimental setup to validate the presented comanipulation approach

The experimental setup consists furthermore of a panel simulating the compression paddle surface and a screen which displays a virtual scene. The robot-probe-panel setup is depicted in figure 11. The screen is placed in front of the subjects and shows the actual position of the US probe with the US plane, as well as its pose with respect to the virtual ROI and the paddle plane. This ROI serves as pointing target and is in reality located within the panel which is placed in front of the robot. In addition a controller was implemented to manage the visual and haptic feedback, i.e. the virtual scene and the force applied by the robot.

### B. Protocol

To validate the principle of co-manipulation a test scenario was developed to perfom a scanning task within a given ROI while focusing on speed and accuracy. The user grasp the probe in its rest position, approaches a ROI and scans it five times from one side to the other and back. During this task the subjects were instructed, once in the ROI, to always intersect the US plane with the ROI of 1cm radius and to perform the task as fast as possible.

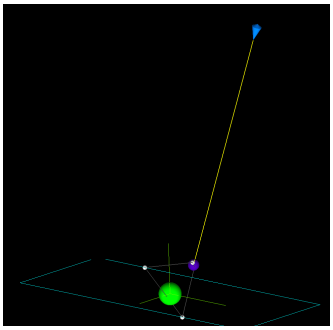

Fig. 11. Virtual scene

The task was conducted with the robot in passive mode (no effort are applied) and with the active robot (with the comanipulation control law). For each of these two configurations, the users were instructed to (re)act in three different ways: keeping a stiff and a soft grasp, as well as reacting intuitively. The latter one was always demanded before the other two ones to assure that the user reacts naturally. Tests were stoped by the investigator when the fifth scanning was completed. When performing the tests with active robot support, the subjects grasp the end-effector to manipulate the probe, see grasp strategy analysis in section III. To simulate and compare to performances of the 6 subjects during a standard US exam without robot comanipulation, they directly handled the probe. In order to eliminate learning effects on test data, the succession of tasks with and without robot assistance was alternated.

To measure the amelioration criteria like duration and precision, the time span of each test as well as the distance from the virtual US plane to the POI was saved and evaluated.

### C. Results and Discussion

The user performances for each of the two system configurations (active or inactive robot) were compared. We distinguished three different grasping strategies: firm, soft and intuitive grasping. For each of those six tests, the time needed to complete the task was clocked. In addition the actual distance between the US plane and the center of the ROI was registered. Based on this data, the average time needed to accomplish a task was computed. Furthermore, the user movement was splited off in two phases: an approaching and a scanning phase. The latter one starts once the US plane enters the ROI. The average plane-target distance was evaluated when the US plane does not intersect the ROI during the scanning phase. In addition the percentage of time frames with plane-target intersection was determined. Table I shows the results for tests using an inactive robot, table II those for an active one.

Comparing the time performances of both configurations, one can state that users were in average more quickly using an active robot. The best average time for an inactive robot test was achieved when intuitively manipulating the probe.

TABLE I

GROUPED TEST RESULTS USING AN INACTIVE ROBOT

| | intuition | soft grasp | firm grasp |
|---|---|---|---|
| average time [ms] | 7291 | 8109 | 7479 |
| average distance to ROI [mm] | 15.52 | 16.46 | 17.37 |
| average time inside ROI [%] | 49.35 | 54.30 | 54.62 |

TABLE II

GROUPED TEST RESULTS USING AN ACTIVE ROBOT

| | intuition | soft grasp | firm grasp |
|---|---|---|---|
| average time [ms] | 6041 | 6854 | 5544 |
| average distance to ROI [mm] | 14.91 | 17.06 | 15.21 |
| average time inside ROI [%] | 58.78 | 54.59 | 53.06 |

An average time of 7.2sec was needed. Nevertheless, this score is below the worst average time span needed for comanipulation tests: 6.8sec for soft grasps. Best average results regarding performance time were clearly achieved for active robot tests when the user has a stiff grasp: 5.5sec.

Analyzing the results for average plane-target distances during the scanning phase when no intersection occurs shows that no real improvement is brought by active robot assistance. For active robot tests when handling intuitively the US probe, an average distance of 15mm was measured in the this phase. This is not considerably better than the worst average distance which was registered for inactive robot test for firm grasps: 17mm.

Regarding the percentage of time frames with plane-ROI intersection, results are similar when indicating the user to adapt a certain grasping strategy during active or inactive robot tests. The average percentage of time frames with intersection is around 54%. Nevertheless, when handling the probe intuitively, one can observe a clear tendency towards better performances using an active robot support, 59% compared to 49%.

The presented results show a slight amelioration using a robot to conduct a scanning task, mainly for intuitive handling. Nevertheless, one have to admit that using a 3D visual interface introduces a bias in favor of the visual feedback. Usually during the medical application only 2D visual feedback is given by displaying the actual US image and a 3D slice reconstruction of the patients' breast. The given 3D visual feedback facilitates the chosen executing task. The visual assistance in this setup is hence higher than in the final application where the US plane is not displayed with reference to the scanning target. The investigator only has a vague idea about the localization of the ROI.

## V. CONCLUSIONS

This paper demonstrates the possibility to provide an adequate task assistance using underactuated robots for human-robot tool comanipulation. The example studied leans on US scans for early breast cancer detection examinations consecutive to DBT scans.

A robot comanipulates the US probe and is programmed to assist the user to make a US scan of a previously defined ROI. In addition it indicates when the US plane is too far away from the ROI. Both, indication and assistance to execute the task, are done by applying a simple force at the robot end effector.

We made use of a PHANToM Omni robot for the implementation of this novel system. In addition, a US probe was rigidly attached on the robot end effector. The probe pose is hence influenced by the user grasp and the robot feedback. Additional visual feedback was given via a screen which displays a virtual scene. The user performances using this novel system to conduct a scanning task were compared to data on usual US scanning without active robot support. Results show that the examination time can be reduced even using underactuated robots. Furthermore, there might be the tendency that scanning accuracy can equally be increased using the presented type of comanipulation robots, but still further tests are necessary.

The next steps of this work are to keep on improving the robot command to optimize the robot-human synergy. Furthermore, the mechanical properties of the used robot have to be revised as well as the test protocol to decrease the bias of 3D visual feedback. Finally, US and DBT data have to be introduced directly to the test setup.

## REFERENCES


[1] P. Cinquin, S. Lavalle, and J. Troccaz, IGOR: Image Guided Operating Robot. Methodology, Applications, EMBS92, pp:1048-1049, 1992.

[2] O. Scheiner, J. Troccaz, O. Chavanon, and D. Blin, PADyC : a Synergistic Robot for Cardiac Puncturing, IEEE ICRA00, pp:2883-2888, april, 2000.

[3] B. Davies, K.L. Fan, R.D. Hibberd, M. Jakopec, and S.J. Harris, A Mechatronic Based Robotic System for Knee Surgery, IEEE Intelligent Information System, pp:48-52, 1997.

[4] E. Bonneau, F. Taha, P. Gravez, and S. Lamy, Surgicobot: Surgical gesture assistance cobot for maxillo-facial interventions, Medical Robotics, Navigation and Visualization, Remagen, Allemagne, march, 2004.

[5] R.H. Taylor, B.D. Mittelstadt, H.A. Paul, W. Hanson, P. Kazanzides, J.F. Zuhars, B. Williamson, B.L. Musits, E. Glassman, and W.L. Bargar, An Image-Directed Robotic System for Precise Orthopaedic Surgery, IEEE Trans. On Robotics an Automation, Vol10(3), pp:261-275, june, 1994.

[6] E. Dombre, G. Duchemin, P. Poignet, and F. Pierrot, Dermarob: a safe robot for reconstructive surgery, IEEE Trans. on Robotics and Automation, Vol19(5), pp:876-884, 2003.

[7] C. Vidal, J.F. Menudet, P. Cinquin, J. Troccaz, G. Morel, J. Szewczyk, J.J. Rambeaud, J.A. Long, and P. Mozer, Projet Rosace: robot scuris d'assistance à la chirurgie endoscopique, IRBM, Vol31, pp:122-126, 2010.

[8] N. Zemiti, T. Ortmaier, M.A. Vitrani, and G. Morel, A force controlled laparoscopic surgical robot without distal force sensing International Symposium on Experimental Robotics, 2004.

[9] R. Taylor, P. Jensen, L. Whitcomb, A. Barnes, R. Kumar, D. Stoianovici, P. Gupta, Z. Wang, E. de Juan, and L. Kavoussi, A steady-hand robotic system for microsurgical augmentation, International Journal of Robotics Research, Vol18 pp:1201-1210, 1999.

[10] M.A.Vitrani, and G. Morel "Hand-Eye Self Calibration of an Ultrasound Image-Based Robotic System", IEEE IROS'08, pp:1179 - 1185, Nice, France, september 2008.